MOLECULAR AND CELLULAR BIOLOGY, Dec. 2000, p. 9212–9224 Vol. 20, No. 24
0270-7306/00/$04.00+0
Copyright © 2000, American Society for Microbiology. All Rights Reserved.

Vav3 Mediates Receptor Protein Tyrosine Kinase Signaling, Regulates GTPase Activity, Modulates Cell Morphology, and Induces Cell Transformation

LIYU ZENG,[1] PALLAVI SACHDEV,[1] LUNBIAO YAN,[2] JOSEPH L. CHAN,[1] THOMAS TRENKLE,[3] MICHAEL MCCLELLAND,[3] JOHN WELSH,[3] AND LU-HAI WANG[1]*

Department of Microbiology, Mount Sinai School of Medicine, New York, New York 10029[1]; Department of Medicine, Columbia University, New York, New York 10032[2]; and Sidney Kimmel Cancer Center, San Diego, California 92121[3]

Received 22 June 2000/Returned for modification 2 August 2000/Accepted 25 September 2000

A recently reported new member of the Vav family proteins, Vav3 has been identified as a Ros receptor protein tyrosine kinase (RPTK) interacting protein by yeast two-hybrid screening. Northern analysis shows that Vav3 has a broad tissue expression profile that is distinct from those of Vav and Vav2. Two species of Vav3 transcripts, 3.4 and 5.4 kb, were detected with a differential expression pattern in various tissues. Transient expression of Vav in 293T and NIH 3T3 cells demonstrated that ligand stimulation of several RPTKs (epidermal growth factor receptor [EGFR], Ros, insulin receptor [IR], and insulin-like growth factor I receptor [IGFR]) led to tyrosine phosphorylation of Vav3 and its association with the receptors as well as their downstream signaling molecules, including Shc, Grb2, phospholipase C (PLC-γ), and phosphatidylinositol 3 kinase. In vitro binding assays using glutathione *S*-transferase-fusion polypeptides containing the GTPase-binding domains of Rok-α, Pak, or Ack revealed that overexpression of Vav3 in NIH 3T3 cells resulted in the activation of Rac-1 and Cdc42 whereas a deletion mutant lacking the N-terminal calponin homology and acidic region domains activated RhoA and Rac-1 but lost the ability to activate Cdc42. Vav3 induced marked membrane ruffles and microspikes in NIH 3T3 cells, while the N-terminal truncation mutants of Vav3 significantly enhanced membrane ruffle formation but had a reduced ability to induce microspikes. Activation of IR further enhanced the ability of Vav3 to induce membrane ruffles, but IGFR activation specifically promoted Vav3-mediated microspike formation. N-terminal truncation of Vav3 activated its transforming potential, as measured by focus-formation assays. We conclude that Vav3 mediates RPTK signaling and regulates GTPase activity, its native and mutant forms are able to modulate cell morphology, and it has the potential to induce cell transformation.

The Vav gene was first identified in gene transfer experiments in hematopoietic cells due to its oncogenic activation (26). Its proto-oncogene product exhibits a characteristic arrangement of structural domains, including an N-terminal calponin homology (CH) domain, an acidic region (AD), a Dbl homology (DH) domain, a pleckstrin homology (PH) domain, a zinc finger (ZF) domain, a proline-rich (PR) region, and two SH3 domains flanking an SH2 domain in its carboxyl terminus (6, 10, 11, 48). Since its discovery, three new Vav members, *Cel* Vav (61) and two mammalian Vavs (Vav2 and Vav3), have been identified (22, 38, 50, 55). Although all Vav family proteins have similar structural features, they display different tissue expression patterns. Vav is primarily expressed in hematopoietic lineages, while Vav2 is ubiquitously expressed (5, 6, 50). Vav3 has a broad but different expression profile compared to that of Vav2 (38, 55).

The biochemical functions of the Vav proteins have been extensively investigated. Among them, the most striking function of the Vav proteins is their guanine nucleotide exchange activity toward small GTP-binding proteins. However, so far, no consensus has been reached concerning the substrate specificities of distinct Vav family proteins (1, 12, 13, 20, 38, 40, 51, 54). Crespo, Bustelo, and their colleagues demonstrated by using baculovirus-derived proteins from Sf9 cells in an in vitro GDP-GTP exchange assay that Vav, once activated, acts as a guanine nucleotide exchange factor (GEF) for Rac-1, Rac-2, and RhoG, to a much lower extent for RhoA, but has no activity for Cdc42 (13, 51). Using the same approach, Bustelo and colleagues reported recently that activated Vav2 but Vav3 are able to catalytically promote guanine nucleotide exchange of RhoA and RhoG, but are much less active toward the Rac proteins. They concluded that both activated Vav2 and Vav3 appear to have no effect on Cdc42 activity (38, 51). In contrast, using bacterially expressed Vav and Vav2 fragments in a similar in vitro assay system, Han et al. reported conflicting observations (20). They observed that an N-terminal truncation mutant of Vav was more active on Cdc42 than Rac-1 or RhoA, and once it was tyrosine phosphorylated by Lck, it had comparable guanine nucleotide exchange activity for Cdc42, Rac-1, and RhoA. In agreement with their in vitro assay, transient transfections of the oncogenic Vav in rat embryo fibroblasts were reported to result in the induction of filopodium formation (20), a morphological change that is mediated by activated Cdc42 (19). Similarly, a bacterially expressed Vav2 fragment containing the DH, PH, and CRD domains was shown to be catalytically more active toward Rac-1 and Cdc42 than RhoA (1), again in conflict with results reported by Movilla and Bustelo (38). Moreover, Olson et al. have also reported Vav-mediated activation of Cdc42 in vivo (40). Beside the fact that different systems were used to synthesize and activate Vav proteins, the reason for these conflicting results is not yet apparent.

Regulation of the Vav proteins appears to involve phosphor-

* Corresponding author. Mailing address: Department of Microbiology, Mount Sinai School of Medicine, New York, NY 10029-6500. Phone: (212) 241-3975. Fax: (212) 534-1684. E-mail: lu-hai.wang@mssm.edu.

ylation and intramolecular interaction. So far, several mechanisms have been observed to be involved in regulating the Vav GEF activities (5). Under physiological conditions, tyrosine phosphorylation of the Vav protein is believed to be critical for activating its GEF activity (13, 20, 35, 51, 54). Phospholipid binding and membrane translocation also have a regulatory effect on the Vav GEF activity (18, 21). Artificial truncation of the CH domain or both CH and AD domains has been shown to lead to constitutive activation of the GEF activity of the Vav protein irrespective of the tyrosine phosphorylation status (5, 25, 51). Interestingly, two other Vav mutants, Vav (Δ1–66) and Vav (Y174F), display enhanced cell-transforming ability and other Vav-mediated cell responses, yet still maintain the phosphorylation-dependent GEF activity (5, 25, 30).

Like other GEFs, Vav proteins harbor the potential to be oncogenically activated. It has been shown by using a focus-formation assay that both Vav and Vav2 could be oncogenically activated by N-terminal truncation (25, 51). However, the oncogenic potential of Vav3 has not been demonstrated so far (38, 55). There also seems to be some controversy over the morphological appearance of foci induced by the different oncogenic Vavs. One group has reported that oncogenic Vav2 induces foci with distinct morphology compared to those of oncogenic Vav, while another group reported that both Vav and Vav2 induce foci with indistinguishable morphology (1, 50).

Consistent with the fact that Vav acts as a Rac GEF (13, 51), several lines of evidence have indicated that Vav can induce activation of Jun N-terminal kinase (JNK) (12, 13, 17, 35, 54), PAK (4), and PIP5-K (42), which are downstream effectors of the Rac protein (59). Stimulation of JNK and PIP5-K by Vav was shown to be mediated by Rac-1 activation (12, 42). In addition, Vav has been shown to activate NF-AT, serum response factor, and NF-κB, leading to gene activation (5, 23, 36, 37, 53, 62). However, the downstream signaling pathways of Vav2 and Vav3 have not been characterized.

All the mammalian Vav proteins have marked effects on cell morphology when overexpressed in rodent fibroblasts. In agreement with its ability to activate Rac and RhoG, Vav induces cell spreading, membrane ruffles, and lamellipodia as well as the formation of an actin ring in the cell periphery (51). Vav2 and Vav3 were also shown to induce extensive membrane ruffles and lamellipodia in NIH 3T3 cells (1, 38, 51).

Parallel with the studies of the GEF activity and downstream signaling of Vav proteins, a great deal of effort has also been devoted to explore the possible upstream regulators of the Vav proteins in response to different environmental stimuli as well as to identify new Vav-interacting partners. So far, most of the studies have been focused on Vav. Collectively, numerous cellular receptors when activated have been shown to be able to mediate a rapid and transient phosphorylation of Vav on its tyrosine residues. Additionally, Jak, Src, and Syk/ZAP70 family cytoplasmic protein tyrosine kinases (PTKs) also appear to be involved in Vav phosphorylation (5, 6, 7, 10, 48).

Aside from the receptor and cytoplasmic PTKs, Vav has also been found to interact with an array of cytoskeletal proteins, cytoplasmic signaling molecules, and nuclear proteins via its SH2 and SH3 domains (10). However, some of these interactions, for example, the association of Vav with insulin receptor (IR), were observed only by in vitro binding experiments using glutathione *S*-transferase (GST) fusion polypeptides (58). Whether these interactions occur under physiological conditions in intact cells remains to be demonstrated. Information on the mechanism of Vav2- and Vav3-mediated signaling is relatively limited. Recently, it was reported that tyrosine phosphorylation of Vav2 was increased upon activation of epidermal growth factor receptor (EGFR) and platelet-derived growth factor receptor (43), and increased phosphorylation of Vav3 was seen upon stimulation of EGFR and T-cell receptor (38).

In view of the distinctive tissue expression patterns of Vav, Vav2, and Vav3, it is likely that they play quite different physiological functions. Recently, Vav knockout mouse models have confirmed the important roles of Vav in early embryonic development as well as in antigen receptor-mediated T- and B-cell proliferation and differentiation (16, 56, 64). Information on the phenotypes of Vav2 or Vav3 knockouts is not yet available.

Our laboratory has been interested in characterizing the biochemical and the biological properties of the oncogene Ros, a receptor protein tyrosine kinase (RPTK). v-*ros* was discovered as the transforming gene carried by an avian sarcoma virus, UR2. The proto-oncogene c-*ros* codes for an RPTK which has high homology with the *Drosophila melanogaster sevenless* protein and the IR family of RPTKs in their PTK domains (8). In this study, we report that human Vav3, a newly identified Ros RPTK interacting partner, displays a broad tissue expression pattern that is distinctive from those of Vav and Vav2. Stimulation of several RPTKs, including EGFR, Ros, IR, and insulin-like growth factor I receptor (IGFR) leads to tyrosine phosphorylation of Vav3 as well as its interaction with the receptors and their downstream signaling molecules. Using an in vitro binding assay of the intracellularly activated GTPases, we also demonstrated the distinct ability of native versus mutant Vav3 in inducing specific small GTPase protein activation. Different upstream RPTKs seem to have distinct regulatory effects on Vav3-mediated activation of the Rho subfamily GTPases, leading to differential morphological changes. Finally, we show that Vav3 harbors transforming potential.

MATERIALS AND METHODS

Plasmids and their construction. (i) GAL4 DNA-BD fusion plasmid. To generate the bait construct, pAS-ros, the cytoplasmic domain of human c-Ros was amplified by PCR with primers 5′-ACGA*CCATGGC*G**AGAAAGATTAAAGAATCAA**-3′ (sense) and 5′-TCTTA*GGATCC*ACGGTA**TTAATCAGACCCAT**-3′ (antisense). The resulting fragment was digested with *Nco*I and *Bam*HI and inserted into the corresponding sites of pAS2-1 (Clontech). Amino acids (aa) 1884 to 2347 of c-Ros were fused to the GAL4 DNA binding domain (aa 1 to 147). In general, the italicized sequences denote the added restriction sites and those in bold denote the sense or antisense sequences of the templates to be amplified.

(ii) pcDNA-Rip (pcRV) and pHEF Vav3SH. A fragment harboring the last 287 aa of human Vav3 (SH3-SH2-SH3) was amplified as described above by using primers 5′-TTAACTA*GCTAGC*ATG**ACTCTGCAGAGAAAGC**-3′ and 5′-GAGCCC*AAGCTT***CATCCTCTTCCACATATG**-3′. The PCR product was digested with *Nhe*I and *Hin*dIII and cloned into the corresponding sites of pcDNA3.1(−)/Myc-His to generate pcDNA-Rip. The 3′ Vav3 fragment was freed from pcDNA-Rip with *Nhe*I and *Pme*I, treated with Klenow I, and cloned into the *Eco*RV site of mammalian expression vector pHEF neo, a human elongation factor promoter-based plasmid containing a *neo* selection marker. The plasmid thus generated was named pHEF Vav3SH, and it encodes the SH3-SH2-SH3 domains of human Vav3.

(iii) pQE-Rip. The prokaryotic expression plasmid pQE-Rip was constructed by PCR using primers 5′-TTGTAGAT*GCATGC***ACTCTGCAGAGAAAGCTAAGG**-3′ and 5′-TTGCCC*AAGCTT***ATTCATCCTCTTCCAC**-3′. The resulting PCR fragment, containing the coding sequence for the last 287 aa of human Vav3, was then digested with *Sph*I and *Hin*dIII and ligated into pQE-30 (QIAGEN Inc.) at the corresponding sites. All in-frame fusions and sequences were confirmed by DNA sequencing.

(iv) pBEF Vav3F, pHEF 5-10, and pHEF 6-10. Full-length Vav3 sequence was freed from pBluescript II KS Vav3-His (55) by *Eco*RI and *Sal*I digestion and cloned into the corresponding sites of the mammalian expression vector pBEF neo to generate pBEF-Vav3F. pBEF neo is similar to pHEF neo except that it contains an internal ribosomal binding site between the Vav3 coding sequence and the *neo* marker. The Vav3 fragment 5-10 (Vav3, bp 338 to 1301) was amplified from pBluescript II KS Vav3-His with primer 5 (5′-CGA*GGTACC*ATGG**CACGACTTTCTCGAACACCT**-3′) and primer 10 (5′-**CTCTTACATACGATCACTGCCAAA**-3′). The Vav3 fragment 6-10 (Vav3, bp 529 to 1301) was generated by PCR with primer 6 (5′-CGA*GGTACC***ATGAAGGCAGAGGAAGC**

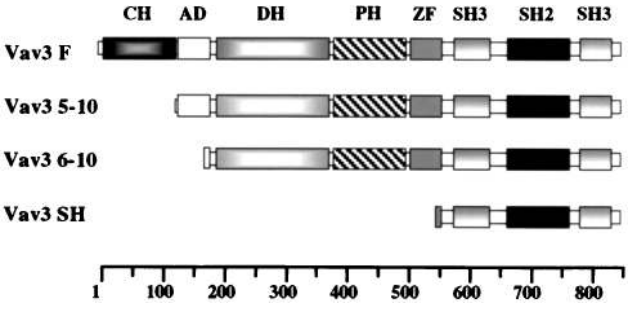

FIG. 1. Schematic diagram of the Vav3 constructs used in biochemical and biological assays.

A-3′) and primer 10. The PCR fragments were cloned into the PGEM-T vector (Promega Corp.). The Vav3 5-10 and 6-10 fragments were subsequently freed using the PGEM-T *Sac*II site and Vav3 *Xba*I site at bp 1233 and inserted into the corresponding sites of pBluescript II KS Vav3-His to replace the 5′ sequence of Vav3 from bp 1 to 1233. The resulting plasmids (named pBluescript II Vav3 5-10 and pBluescript II Vav3 6-10, respectively) were digested with *Kpn*I and *Bam*HI. The freed fragments encoding aa 114 to 590 and aa 177 to 590 of Vav were inserted into the corresponding sites of pHEF-Vav3SH, generating pHEF 5-10 encoding Vav3 aa 114 to 847 and pHEF 6-10 encoding Vav3 aa 177 to 847, respectively (Fig. 1).

pCDNA3.1 ER2 (encoding an EGFR and Ros chimera) and pHEF IR and pHEF IGFR (encoding the full-length cDNA of IR and IGFR, respectively) were constructed in our laboratory.

The *Escherichia coli* expression vector pGEX-GST-Pak CRIB (Cdc42 and Rac interactive binding) that contains the p21 (Cdc42/Rac1) binding domain (PBD) of human Pak1 (aa 70 to 132) was a gift from Bruce Mayer (Howard Hughes Medical Institute, Children's Hospital). The *E. coli* expression vector pGEX-2TH-GST-ACK42 containing the Cdc42 binding domain of human Ack-1 (aa 504 to 545) was a gift from Hiroshi Maruta (Ludwig Institute for Cancer Research). pGEX-4T2-GST-Rok containing the Rho-binding domain of Rok-α (aa 809 to 1062) was generated by PCR from Rok-α cDNA, which was a gift from Thomas Leung and Ed Manser of the Glaxo-IMCB Laboratory, Institute of Molecular and Cellular Biology, Singapore, Singapore. A 5′ primer (5′-GGG*GATCC***AACACCCTAAAAATGTCA**-3′) containing a *Bam*HI site at the 5′ end and a 3′ primer (5′-GGGCCG*GAATTC***CTTAAGCTCCATATGTAA**-3′) containing an *Eco*RI site were used to amplify the region between aa 809 and 1062 of the Rok-α cDNA. The subsequent PCR fragment was cloned into a PGEM-T vector. The insert was released using *Bam*HI and *Eco*RI and inserted into the corresponding sites in pGEX-4T2.

Yeast two-hybrid screening. A yeast two-hybrid system with both *lacZ* and His3 selections (2, 15) was used. CG1945 and Y190 cells (Clontech) transformed with the pAS-ros bait produced an expected 69-kDa fusion protein detected by Western blotting with an antibody against the GAL4 DNA-binding domain (Upstate Biotechnology Inc. [UBI]). CG1945 cells transformed with the bait construct were then transformed with DNA from a human placenta cDNA library (Clontech) by the lithium acetate method (24). To identify positive clones, the colony-lift β-galactosidase filter assay was performed according to Clontech's manual.

Cells and DNA transfection. Human embryonic kidney (HEK) 293T, NIH 3T3, EB69 (a stable NIH 3T3 cell line overexpressing ER2, an EGFR-Ros chimera), and 3T3 IR and 3T3 IGFR (IR- and IGFR-overexpressing NIH 3T3 cell lines, respectively) cells were maintained in Dulbecco modified Eagle medium (DMEM) with 10% calf serum. Calcium phosphate and liposomal transfection methods were used in coimmunoprecipitation and immunofluorescence assays, respectively.

Antibodies. A polypeptide containing the SH3-SH2-SH3 domains of Vav3 and an affinity tag consisting of six consecutive histidine residues (six-His tag) were expressed in the K-12-derived *E. coli* strain M15[pREP4], transformed with pQEVav3SH, and purified by using Ni-nitrilotriacetic acid resin. The purified polypeptide was then used to generate rabbit polyclonal anti-Vav3 antibody. Anti-Ros, anti-IR, anti-IGFR, and anti-IRS-1 antibodies were made in our laboratory. Anti-EGFR antibody for immunoblot assays was a gift from P. Fedi (DHRCC, Mount Sinai School of Medicine). Anti-EGFR antibody for immunoprecipitation was purchased from Santa Cruz Biotechnology. Anti-Shc, anti-Grb2, anti-phosphotyrosine-RC20 conjugated to horseradish peroxidase (HRP), goat anti-rabbit immunoglobulin G (IgG)-HRP, and goat anti-mouse IgG-HRP antibodies were purchased from Transduction Laboratories. Anti-p85 phosphatidylinositol 3 (PI3) kinase polyclonal antibody was purchase from UBI. Anti-hemagglutinin (HA) monoclonal antibody 12CA5 was obtained from the Mount Sinai Hybridoma Core facility.

Northern blot analysis. Human Multiple Tissue Northern (MTN) Blots (samples 7759-1 and 7760-1) and Express Hyb Hybridization Solution were purchased from Clontech Laboratories Inc. A 600-bp *Pst*I fragment corresponding to the N-SH3-SH2 domain of Vav3 was labeled with [α-^{32}P]ATP with a specific activity of 7×10^8 to 9×10^8 cpm/μg and was used as a probe, and a 2.0-kb human β-actin cDNA (Clontech) was used as a probe for the loading control of mRNAs. Prehybridization and hybridization were performed at 68°C for 1 h and washed with 0.1× SSC–0.1% sodium dodecyl sulfate (SDS) at 50°C (1× SSC is 0.15 M NaCl and 0.015 M sodium citrate). Autoradiography was performed for 1 h to 4 days using Kodak XAR5 X-ray film. After stripping with 0.5% SDS at 90 to 100°C for 10 min, the blots were reprobed at room temperature for 1 h with a Vav3-specific oligonucleotide probe, corresponding to nucleotides 1722 to 1751 of Vav3 (5′-CGCAGTCCATTGGTCCGTTTCTCTGGTAGT-3′). The blots were then washed with 2× SSC–0.05% SDS and 0.1× SSC–0.1% SDS at room temperature for 40 min each, covered with plastic wrap, and exposed to X-ray film at −70°C.

Protein analysis. Thirty-two hours after transfection, cells were serum starved for 16 h and treated for 15 min with EGF (100 ng/ml), insulin (50 nM), or IGF-1 (100 ng/ml). Cells were lysed in Nonidet P-40 (NP-40) buffer (20 mM Tris-HCl [pH 7.4] 150 mM NaCl, 5 mM EDTA, 1% NP-40, 10% glycerol, 1 mM sodium vanadate, 1 mM phenylmethylsulfonyl fluoride, and 1% Trasylol), and equivalent amounts of protein were incubated with respective primary antibodies overnight at 4°C, followed by incubation with protein A-Sepharose for 1 h. The beads were washed three times in the NP-40 buffer, resuspended in the appropriate volume of Laemmli buffer, and subjected to SDS-polyacrylamide gel electrophoresis. The proteins were electrotransferred to nitrocellulose membranes and blocked in 5% milk or 1% bovine serum albumin in TBST buffer (Tris-buffered saline [pH 7.5], 1% Tween 20) overnight. Blocked filters were probed with primary antibodies in the same buffer, followed by secondary antibody conjugated to HRP in blocking solution, and then filters were developed using enhanced chemiluminescence (ECL) detection (Amersham Pharmacia Biotech).

Assay of activated RhoA, Rac-1, and Cdc42. The synthesis of the fusion polypeptides GST–Rok-α (aa 809 to 1062), GST-Ack42 (aa 504 to 545), and GST-Pak CRIB (aa 70 to 132) encoded in their respective plasmids was induced in *E. coli* cells with 0.4 mM isopropyl-β-D-thiogalactopyranoside (IPTG) at 30°C for 4 h, and proteins were affinity purified using a 50% slurry of glutathione-Sepharose 4B (Amersham Pharmacia Biotech) according to the Batch Purification method provided by the manufacturer. The glutathione-Sepharose beads conjugated with GST-Pak, GST-Ack42, or GST–Rok-α were used as specific probes for in vitro binding assays of activated Rac-1, Cdc42, and RhoA, respectively.

NIH 3T3 cells or NIH 3T3 cells overexpressing IR or IGFR were transiently transfected with phEF HA-tagged wild-type Rac, wild-type Rho, or wild-type Cdc42 along with the control vector phEF, phEF Vav3F, or phEF 6-10. At 24 h posttransfection, the cells were starved overnight in serum-free DMEM and then were left untreated or stimulated with the appropriate ligand for 15 min. Cells were lysed in 1% NP-40 extraction buffer containing 10 mM $MgCl_2$. Samples of 500 μg of protein lysate from various transfected cells were mixed with 20 μg of GST-Pak CRIB, GST–Rok-α, or GST-Ack42 beads and incubated at 4°C for 2 h. The beads were washed three times in lysis buffer and analyzed by Western blotting to detect the bound GTPases. HA-tagged Rac-1, RhoA, and Cdc42 were detected with anti-HA monoclonal antibody 12CA5. The primary antibody was detected with HRP-coupled anti-mouse IgG antibody using ECL.

Immunofluorescence staining. Parental NIH 3T3 cells were seeded 1 day before transfection. Transient transfection was performed the next day at a 60 to 80% cell confluency using Lipofectamine Plus (Gibco BRL). Then, 24 h later, cells were trypsinized, counted, and seeded onto coverslips placed in 35-mm-diameter dishes at a density of 10^5 cells/dish and were allowed to grow for another 24 h in DMEM with 10% calf serum. In some cases, cells were serum starved for 12 to 16 h before being subjected to fixation and subsequent staining to lower the background in control cells. Cells were washed twice with 1× Hanks balanced salt solution (Gibco BRL) and fixed in 2% paraformaldehyde–0.1% glutaraldehyde–0.05% Triton X-100 at room temperature for 20 min. After rinsing with 1× Hanks solution three times, the coverslips were blocked with 1% bovine serum albumin–1% phosphate-buffered saline for 30 min. Cells were incubated with anti-Vav3 antibody for 2 h followed by three washes with 1× Hanks solution, followed by incubation with anti-rabbit secondary antibody coupled to fluorescein isothiocyanate alone or along with rhodamine-labeled phalloidin for 1 h. Following three washes in 1× Hanks solution, the coverslips were mounted on microscope slides by using the ProLong Antifade Kit (Molecular Probes) and were examined under the fluorescence microscope.

Focus formation assay. Samples with 2×10^5 NIH 3T3 cells were seeded into 10-cm-diameter dishes in DMEM with 10% calf serum 24 h prior to transfection. The cells were transfected using the calcium phosphate method. At 10 to 12 h posttransfection, the cells were washed once with serum-free DMEM and then maintained in DMEM with 5% calf serum. Ten to 14 days later, cells were fixed in 70% ethanol at room temperature for 20 min, air dried for 30 min, and then stained with Giemsa stain (Sigma Diagnostics) at 37°C for 45 to 60 min. After washing two times with 1× phosphate-buffered saline, cells were air dried and foci were enumerated.

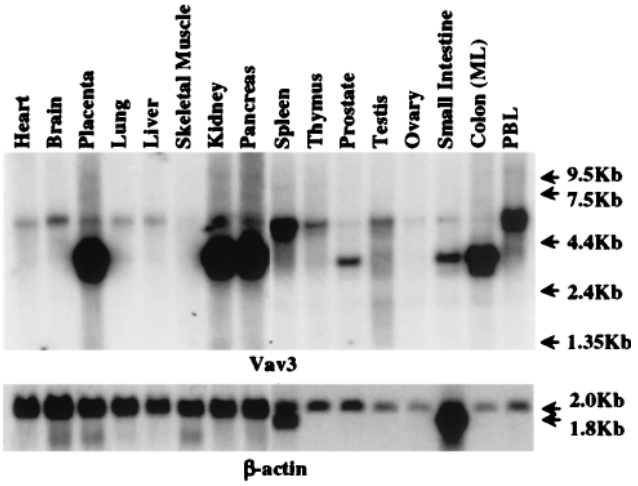

FIG. 2. Northern blot analysis of Vav3 transcripts. A *Pst*I-*Pst*I fragment of Vav3 which included the N-terminal SH3 and SH2 domains was labeled with [α-^{32}P]ATP and used as the probe. Human Multiple Tissue Northern (MTN) Blots (Clontech) (samples 7759-1 and 7760-1) were prehybridized and hybridized in Express Hyb Hybridization Solution at 68°C as described in the manufacturer's manual. Human β-actin cDNA (Clontech) was used as a control probe for monitoring the quantities of mRNAs.

RESULTS

Identification of Vav3 as Ros-interacting protein. To identify potential novel molecules implicated in Ros-mediated signaling pathways, we screened a human placenta cDNA library using the cytoplasmic domain of human c-Ros as bait in a yeast two-hybrid assay. Of the 5×10^6 transformants, 52 conferred upon the CG1945/pAS-Ros cells the ability to grow on SD/−Trp/−Leu/−His/+3-AT plates and to produce β-galactosidase. Of these, 32 colonies were determined as "true" positive based on the criterion that they could not induce His or β-galactosidase production when mated to Y187 cells carrying pAS2-1 or pLAM5′. One of the positive cDNA isolates was found to represent a novel sequence at the time of identification and was later shown to encode the carboxyl SH3-SH2-SH3 domains of Vav3, a newly identified Vav homologue (data not shown).

Tissue expression pattern of Vav3. Northern blot analysis revealed two main species of human Vav3 mRNA transcripts, 5.4 and 3.4 kb, which are broadly distributed in most of the hematopoietic and nonhematopoietic tissues except ovary and skeletal muscle (Fig. 2). Placenta, kidney, pancreas, and colon cells express the highest levels of the 3.4-kb transcript. The larger Vav3 mRNA is present at an intermediate level in spleen cells and peripheral blood lymphocytes (PBLs). The probe generated using the C-terminal SH3 and SH2 domains may potentially recognize the highly homologous domains of the other Vav family members and therefore may complicate the interpretation of our observed results. However, the specificity of the probe toward Vav3 but not Vav was demonstrated by its inability to detect the Vav transcripts (2.9 kb) in Vav-rich tissues (spleen, thymus, lung, and PBL). Additionally, the 5.4-kb Vav3 transcript was detected at a high level in spleen cells but at a low level in placenta and liver cells, whereas Vav2 mRNA transcripts (5 kb) displayed comparable levels in these tissues (50), leading us to believe that a possible cross-reaction of our Vav3 probe with Vav2 transcripts is unlikely. Furthermore, the Vav3 mRNA expression pattern was confirmed by using a Vav3-specific oligonucleotide probe to hybridize with the same filters (data not shown).

The distribution pattern of the larger Vav3 transcript is similar to that observed by Movilla and Bustelo (38). However, in their study, they observed only the larger Vav3 transcript in human tissues. One possible reason for their failure to detect the smaller Vav3 transcript is that they used a probe that did not include the SH3-SH2-SH3 domains of Vav3. Using that probe, they did not detect Vav-1- or Vav-2-related transcripts at the size of 3.1 kb either. The smaller Vav3 mRNA detected here is most likely equivalent to the major variant transcript of Vav3 (3.1 kb) that contains only the SH3-SH2-SH3 domains that were reported previously (55). In that study, the variant transcript of Vav3 was found, by reverse transcription-PCR, to be preferentially expressed in placenta, kidney, pancreas, colon, small intestine, and prostate cells (55), which is similar to our present observation (Fig. 2).

Tyrosine phosphorylation of Vav3 and its interaction with RPTKs and their signaling molecules. To investigate the biochemical functions of Vav3, expression vectors containing the SH3-SH2-SH3 region (Vav3SH) or full-length Vav3 (Vav3F) were generated as stated in Materials and Methods. To confirm the interaction of Vav3 with Ros in mammalian cells, 293T cells were transiently transfected with ER2 (EGFR-Ros chimera) and Vav3SH. Vav3SH was tyrosine phosphorylated in ER2-transfected 293T cells, and the level of phosphorylation was enhanced upon activation of Ros; however, its association with Ros was constitutive (Fig. 3A). Coexpression of Vav3F and ER2 in 293T cells resulted in a significantly higher level of tyrosine phosphorylation of Vav3 than Vav3SH (data not shown), suggesting that the majority of phosphotyrosine sites of Vav3 may be distributed in its N-terminal and central regions. The SH3-SH2-SH3 domains of Vav3 seem to be sufficient in mediating the interaction of Vav3 and Ros, as evidenced by the reciprocal immunoprecipitation and Western blotting (Fig. 3A). Furthermore, an ER2-overexpressing NIH 3T3 cell line (EB69) was used to investigate Vav3 phosphorylation and interaction with Ros. In this system, the tyrosine phosphorylation of Vav3 was clearly ligand dependent, but the association of Vav3 and Ros was still constitutive (Fig. 3B). In contrast, upon activation of the endogenous EGFR in 293T cells, Vav3 was rapidly tyrosine phosphorylated and associated with EGFR in a ligand-dependent manner (Fig. 3C). Since IR and IGFR have high homology with Ros in their PTK domains, we tested whether Vav3 can also interact with these receptors. Constructs encoding the full-length cDNA of IR or IGFR were cotransfected with either Vav3F or Vav3SH. The full-length Vav3 protein and its carboxyl SH3-SH2-SH3 fragment were tyrosine phosphorylated in response to insulin stimulation, although the former had a significantly higher phosphorylation level (Fig. 4 and 5). Increased association between Vav3 and IR was observed upon insulin stimulation (Fig. 4). Although no significant tyrosine phosphorylation of Vav3SH was detected (Fig. 5A), phosphorylation of Vav3F, Vav3 5-10, and Vav3 6-10 was significantly enhanced (Fig. 5B) in response to IGF-1 stimulation. Similarly, increased association of IGFR with Vav3F, Vav3 5-10, and Vav3 6-10 was observed upon IGF-1 stimulation, indicating that the interaction does not require the N-terminal domain. Upon IR or IGFR activation, two Vav3-associated proteins (180 and 97 kDa) were found to be heavily tyrosine phosphorylated (Fig. 4 and 5A). Reprobing the respective filters with anti-IR or anti-IGFR antibody revealed that the 97-kDa proteins were the β subunits of IR and IGFR, respectively. The 180-kDa Vav3-associated protein was also found in the anti-Vav3 phosphotyrosine blots upon Ros and EGFR activation (Fig. 3 to 7). We repeatedly observed that the 180-kDa protein remains the most prominent Vav3-associated tyrosine-phosphorylated protein upon activation of various

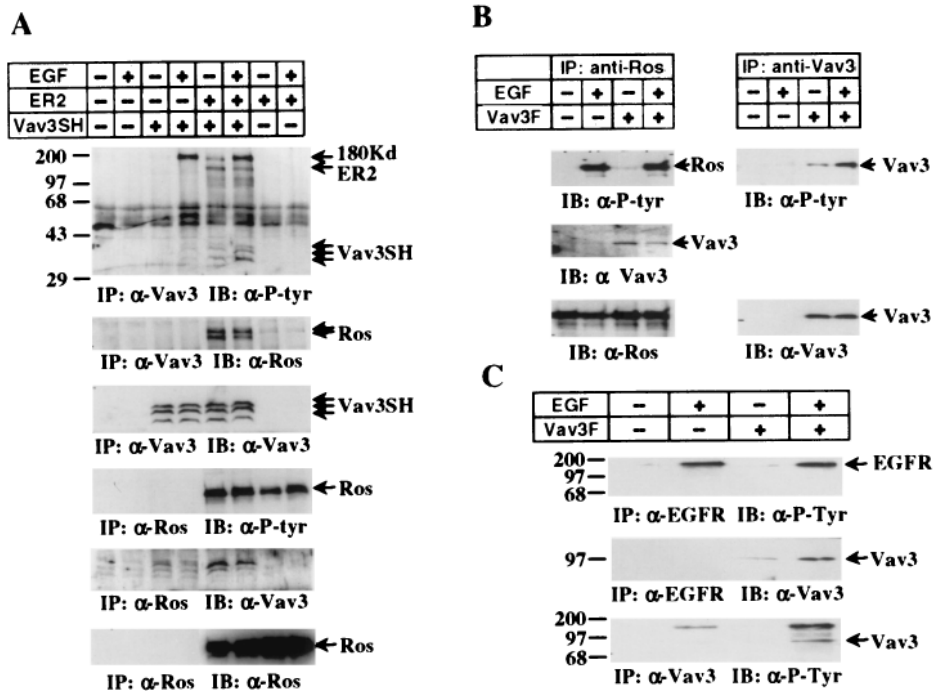

FIG. 3. Vav3 is tyrosine phosphorylated by Ros and EGFR and interacts with these receptors. (A) Samples of 100 ng of ER2 and 10 μg of Vav3SH were cotransfected into 293T cells as indicated. After serum starvation and treatment for 15 min with 100 ng of EGF/ml, cells were lysed and subjected to immunoprecipitations (IP) and Western blotting (IB). EB69 cells (B) and 293T cells (C) were transfected with either empty vector pHEF neo or Vav3F. Vav3 was immunoprecipitated with anti-Ros or anti-EGFR antibodies. The tyrosine phosphorylation of Vav3 was visualized by immunoprecipitation with anti-Vav3 antibody and Western blotting with anti-phosphotyrosine antibody.

RPTKs that we have examined so far. Although anti-Ros, anti-EGFR, anti-IRS-1, and anti-p190 Rho-GAP antibodies were used in an effort to characterize the protein, the identity of the protein remains unknown.

We next examined the interaction of Vav3 with several downstream signaling molecules implicated in Ros-, IR-, and IGFR-mediated signaling pathways, including Shc, Grb2, phospholipase C (PLC-γ), and the regulatory subunit p85 of

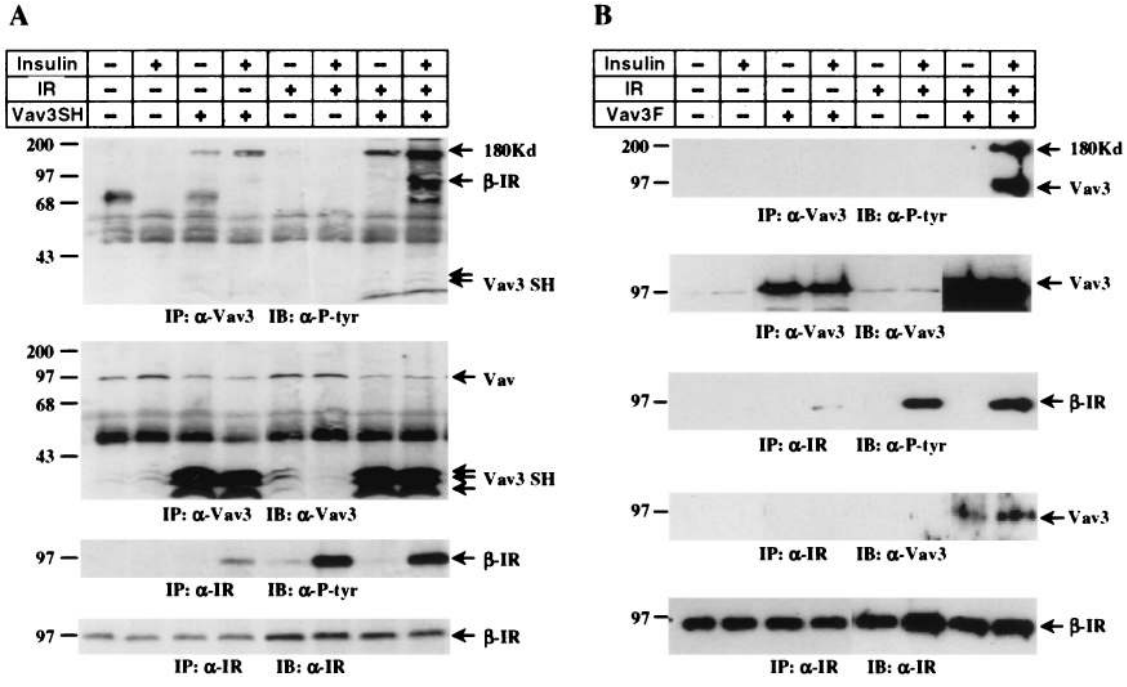

FIG. 4. Vav3 is tyrosine phosphorylated and associates with the IR upon its activation. 293T cells were transfected with 10 μg of Vav3SH (A) or 10 μg of Vav3F (B) in the absence or presence of exogenously transfected IR (100 ng). A sample of 1 mg of total-cell lysate was used in the immunoprecipitations (IP) and Western blottings (IB) as indicated.

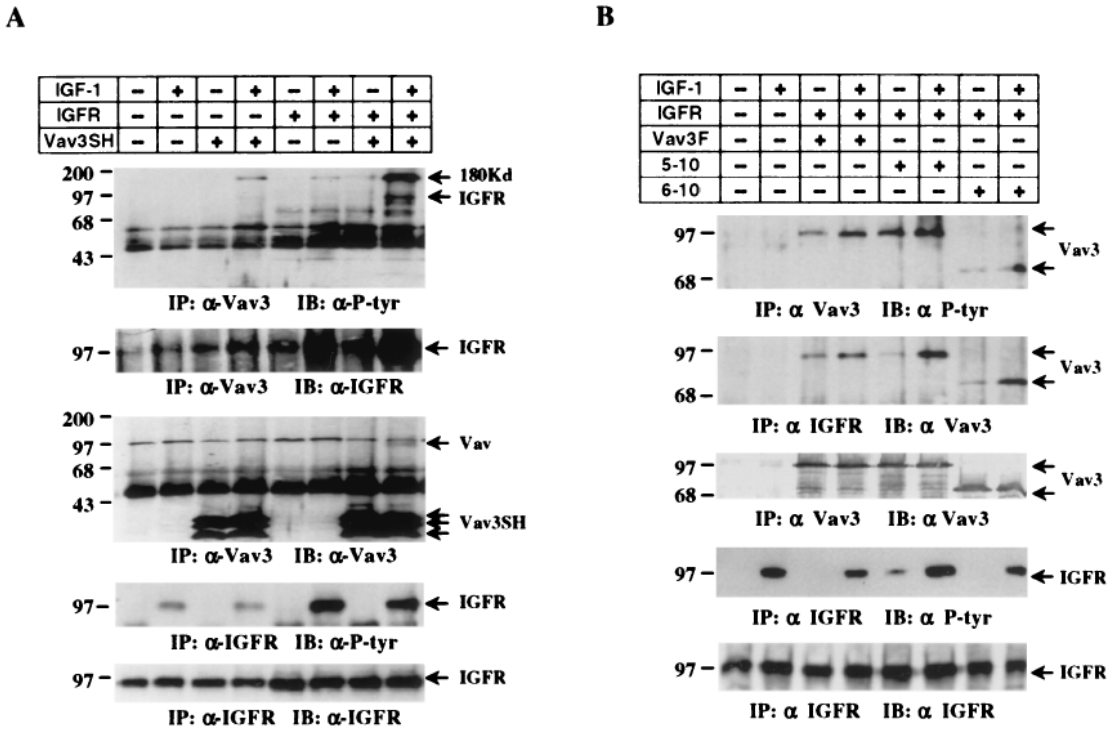

FIG. 5. Vav3 becomes tyrosine phosphorylated and interacts with the IGF-1 receptor upon IGF-1 stimulation. Samples of 100 ng of pHEF IGFR and 10 μg of Vav3SH (A) or 10 μg of Vav3F, Vav3 5-10, or Vav3 6-10 (B) were used in cotransfections of 293T cells. Vav3 and IGFR were immunoprecipitated (IP) from 1 mg of total-cell lysate and subjected to Western blotting (IB) as indicated.

PI3 kinase. As shown in Fig. 6, Vav3 interacted with PLC-γ (Fig. 6A) and PI3 kinase p85 (Fig. 6B) upon EGF stimulation in EB69 cells overexpressing the EGFR-Ros chimera. As expected, IRS-1 associated with p85 in response to activation of the Ros chimera (Fig. 6C). The association of Vav3 with p85 was confirmed by coimmunoprecipitation with anti-p85 antibody (Fig. 6C). The association of Vav3 with the p85 subunit of PI3 kinase in EB69 cells and parental NIH 3T3 cells upon EGF, insulin, and IGF-1 stimulation was further confirmed by in vitro PI3 kinase assays (data not shown). Vav3 associated with Grb-2 in an insulin-dependent manner in 293T cells transiently expressing Vav3F (Fig. 7). The interaction of Vav3 with Grb-2 was, as expected, further enhanced in the presence of exogenously introduced IR. Vav3 was found to interact with Shc in an insulin-dependent manner as well (Fig. 7).

Overexpression of Vav3 and its mutants in NIH 3T3 cells leads to activation of Rho family GTPases. Since Vav and Vav2 have guanine nucleotide exchange activity towards Rho family GTPases, we decided to characterize the possible effect of Vav3 on Rho, Rac, and Cdc42 proteins. In view of the conflicting results produced using bacterium- or baculovirus-derived Vav proteins in the in vitro GTP-GDP exchange assays (1, 12, 13, 20, 38, 51), we used the newly developed Rok, Pak, and Ack in vitro binding assays described in Materials and Methods to detect the levels of intracellular activated forms of RhoA, Rac-1, and Cdc42. Rok-α, Pak, and Ack GST fusion

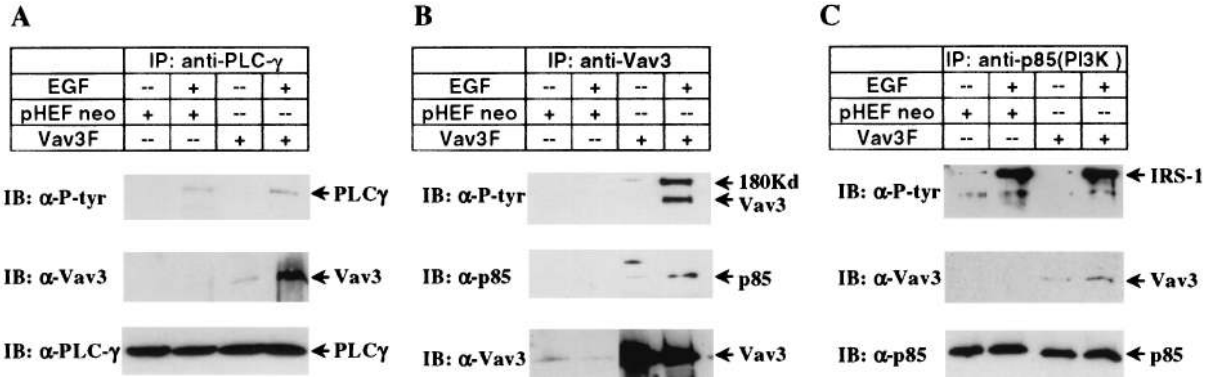

FIG. 6. Vav3 associates with PLC-γ and PI3 kinase p85 in ER2-expressing NIH 3T3 cells (EB69). EB69 cells were transfected with either Vav3F (10 μg) or pHEF neo (10 μg) as a control. At 48 h posttransfection, cells were stimulated with EGF (100 ng/ml) for 15 min and lysed. A sample of 1 mg of total-cell lysate was used in immunoprecipitations (IP) and Western blottings as indicated.

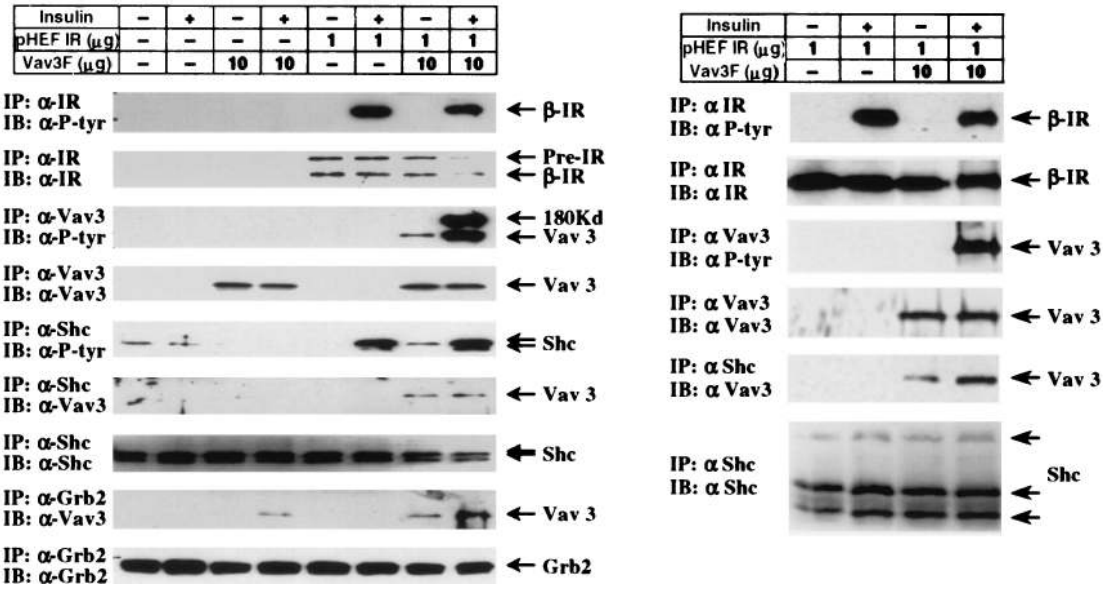

FIG. 7. Vav3 interacts with Shc and Grb-2 in IR-overexpressing 293T cells. Cotransfections were performed with 293T cells as indicated. A sample of 1 mg of lysate with or without insulin stimulation was immunoprecipitated (IP) with anti-Grb2 or anti-Shc antibody, followed by Western blotting (IB) with anti-Vav3 antibody. The tyrosine phosphorylation level of IR and Vav3 as well as the protein amounts of IR, Vav3, Shc, and Grb2 were determined by immunoprecipitation and Western blotting with antibodies against phosphotyrosine and these proteins, respectively.

proteins containing the respective Rho binding domain or CRIB domain have previously been shown to specifically bind to the active GTP-bound forms of RhoA, Rac-1, and Cdc42, respectively (27, 32, 39, 49). NIH 3T3 cells were transiently transfected with various Vav3 constructs along with HA-tagged wild-type RhoA, Rac-1, or Cdc42. The ability of the wild-type Vav3 or its mutant, Vav3 6-10, to promote Rho family GTPases activation was determined by the amount of specific Rho GTPase bound by GST-Rok, Pak, or Ack immobilized on glutathione beads, respectively. Figure 8 shows that overexpression of the wild-type Vav3 in NIH 3T3 cells led to a marked activation of Rac-1 and Cdc42 (Fig. 8B and C), but no detectable activation of RhoA (Fig. 8A). The CH-AD domain deletion mutant of Vav3 (6-10), in contrast, was unable to activate Cdc42 (Fig. 8C), but promoted significant activation of RhoA and Rac-1 (Fig. 8A and B).

Since activation of IR or IGFR led to tyrosine phosphorylation of Vav3 (Fig. 4 and 5), we investigated whether these RPTKs could promote Vav3-mediated Rho, Rac, and Cdc42 activation. For this purpose, HA-tagged wild-type GTPases were cotransfected with Vav3F into 3T3-IR or 3T3-IGFR cells. At 24 h posttransfection, the cells were starved for 16 to 20 h and then stimulated with their respective ligands for 15 min. Cell lysates were prepared and used for in vitro binding assays as described above. As shown in Fig. 9, insulin could promote activation of Rac-1 and Cdc42 in 3T3-IR cells, even in the

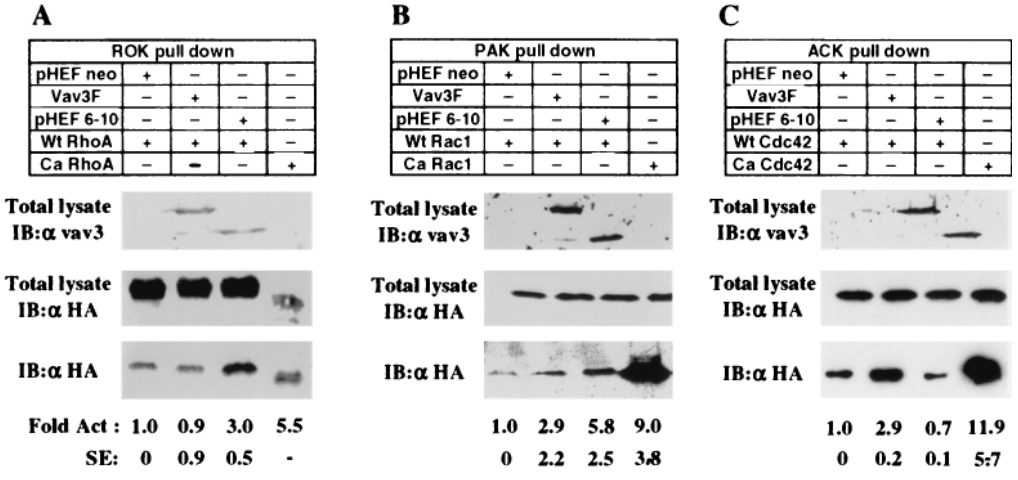

FIG. 8. Activation of GTPases by Vav3 and its mutant 6-10. Vav3F (1.5 μg) and pHEF 6-10 (1.5 μg) were cotransfected with HA-tagged wild-type RhoA (A), Rac-1 (B), or Cdc42 (C) (0.5 μg each) into NIH 3T3 cells. Then, 36 h later, cells were serum starved overnight and extracted in NP-40 lysis buffer. A sample of 500 μg of total-cell lysate was used in Rok-, Pak-, and Ack-GST binding assays as described in Materials and Methods. The data from three independent experiments were normalized for protein expression. The average fold activation (Fold Act) of the respective GTPase and the standard error (SE) were calculated and are presented along with a representative blot. Ca, constitutively activated.

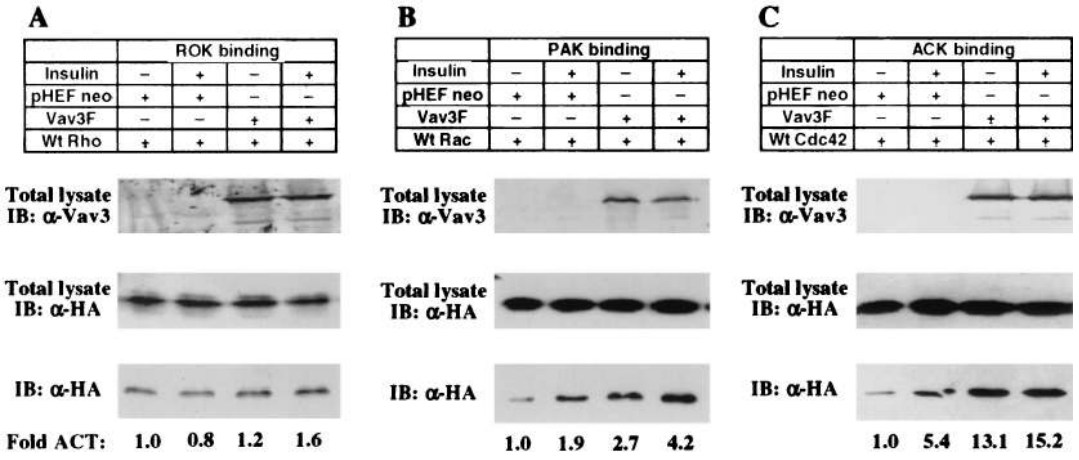

FIG. 9. Insulin enhances Vav3-mediated Rac-1 activation. Empty vector or Vav3F was cotransfected with HA-tagged wild-type RhoA (A), Rac-1 (B), or Cdc42 (C) into NIH 3T3 cells overexpressing IR. After cells were treated with 50 nM insulin for 15 min, they were extracted using NP-40 buffer and subjected to Rok-, Pak-, and Ack-GST pull-down assays. The data from two independent experiments were normalized for protein expression. The average fold activation (Fold ACT) of the respective GTPase was calculated and is presented along with a representative blot.

absence of exogenous Vav3. Introduction of exogenous Vav3 enhanced Rac and Cdc42 activation in a ligand-dependent (for Rac) or ligand-independent (for Cdc42) manner (Fig. 9B and C). Vav3 had little effect on RhoA with or without insulin stimulation (Fig. 9A). Vav3-enhanced activation of Rac-1 in response to insulin was also observed in Cos-7 cells (data not shown). In 3T3-IGFR cells, coexpression of Vav3 slightly enhanced Rac-1 and RhoA activation in a ligand-independent manner and had a significant synergistic effect on IGF-1-induced Cdc42 activation (Fig. 10B).

Our results suggest that IR activation enhanced the ability of Vav3 to promote Rac-1, but not RhoA and Cdc42, activation although Vav3 significantly increased the level of activated Cdc42 without insulin stimulation, whereas IGFR promoted Vav3-mediated Cdc42, but not RhoA and Rac-1, activation. However, since NIH 3T3 cells express an undetectable level of endogenous Vav3, the role of Vav3 in IR and IGFR signaling in 3T3 cells remains unclear.

The effect of Vav3 and its mutants on the morphology of NIH 3T3 cells. To determine if Vav3 activation of the Rho family GTPases results in changes in cell morphology, we transiently transfected wild-type Vav3 into NIH 3T3 cells and performed immunofluorescence staining as described in Materials and Methods. As shown in Fig. 11, Vav3 was exclusively distributed in the cytoplasm, particularly surrounding the perinuclear area. Subcellular fractionation revealed that the majority of Vav3 protein was located in the cytosolic fraction (data not shown). Parental NIH 3T3 cells and Vav3SH-transfected cells predominantly displayed fibroblast-like morphology (Fig. 11, top row). A high proportion of wild-type Vav3-overexpressing cells appeared enlarged and frequently multinucleated, usually accompanied by pronounced membrane ruffles and microspikes (Fig. 11, second row). Costaining the cells with anti-Vav3 antibody and rhodamine-conjugated phalloidin revealed that Vav3F induced actin reorganization to form enriched circular actin bundles around the perimembrane area (data not shown). Vav3-positive cells with altered cell shape exhibited three typical cell characteristics: membrane ruffles, membrane ruffles plus microspikes, or microspikes alone. The percentages of Vav3-positive cells with these shapes were found to be 14,

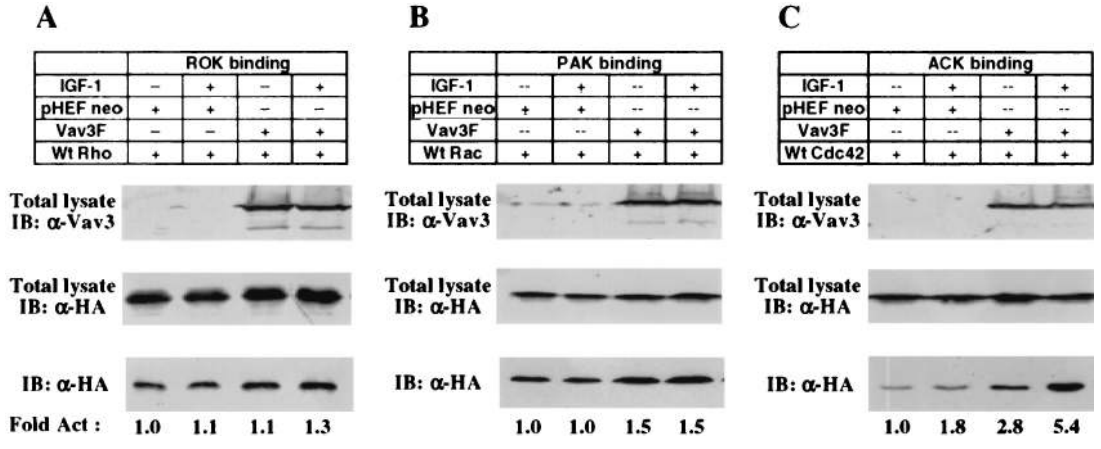

FIG. 10. IGF-1 enhances Vav3-mediated Cdc42 activation. Empty vector or Vav3F was cotransfected with HA-tagged wild-type RhoA (A), Rac-1 (B), or Cdc42 (C) into NIH 3T3 cells overexpressing IGFR. Cells were treated with 100 ng of IGF-1/ml for 15 min and extracted using NP-40 buffer followed by Rok-, Pak-, and Ack-GST pull down assays. The data from two independent experiments were normalized for protein expression. The average fold activation (Fold Act) of the respective GTPase was calculated and is presented along with a representative blot.

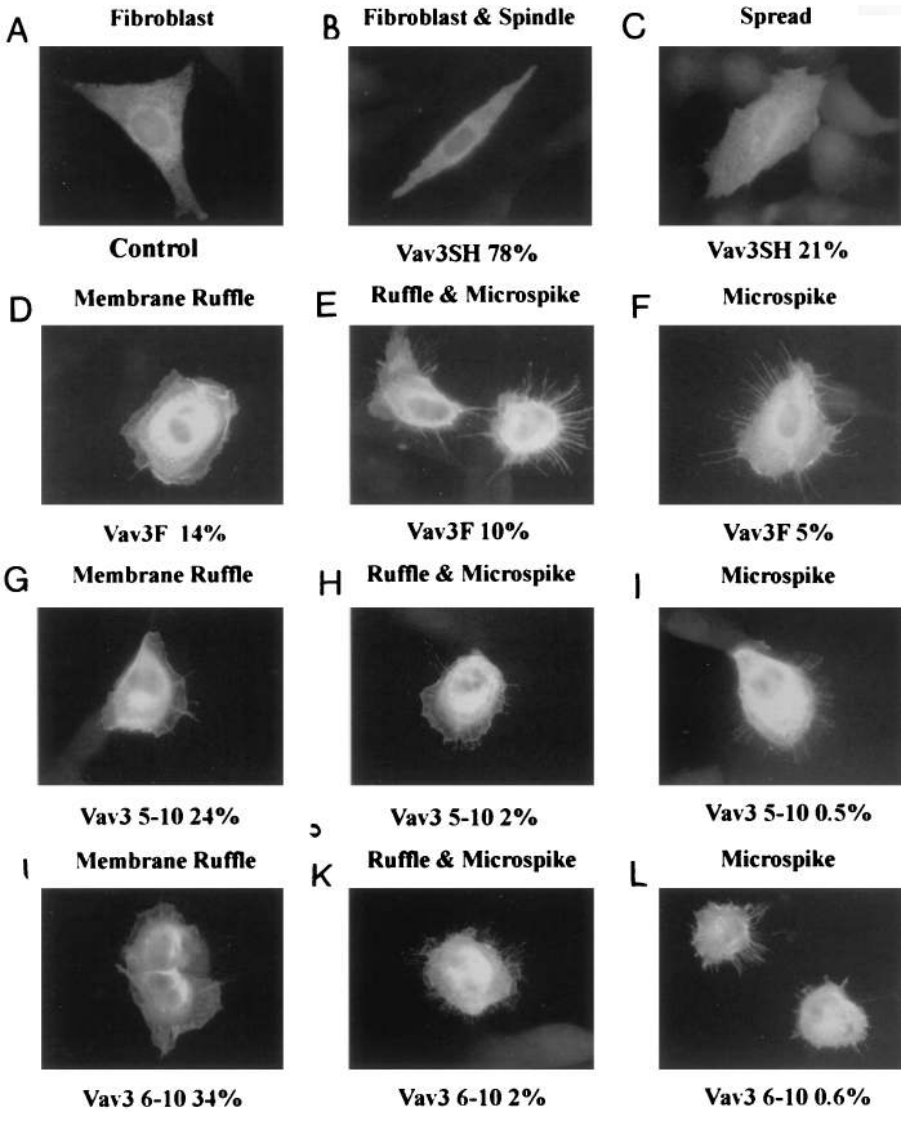

FIG. 11. Effect of Vav3 and its mutants on the morphology of NIH 3T3 cells. NIH 3T3 cells transfected with 2 μg of pEGFP C1 (clontech) (A), Vav3SH (B and C), Vav3F (D to F), pHEF5-10 (G to I), or pHEF6-10 (J to L) were fixed and visualized by staining with anti-Vav3 antibody and subsequently anti-rabbit secondary antibody coupled to fluorescein isothiocyanate (FITC). The proportion of positive cells with distinct morphology in the absence of serum is under the corresponding panels.

10, and 5%, respectively, in the absence of serum. In contrast, the N-terminal truncation mutants, 5-10 and 6-10, of Vav3 dramatically enhanced membrane ruffle formation (24 and 34%, respectively, in the absence of serum), but lost the ability to induce microspikes (Fig. 11, third and fourth rows). Less than 1% of the control and Vav3SH-transfected cells displayed extensive membrane ruffles or microspikes. It is interesting that unlike its homologues Vav and Vav2, Vav3 does not require oncogenic activation for the induction of morphological changes, although the presumed activated forms of Vav3 appear to have increased ability to induce membrane ruffles.

To study the role of Vav3 in RPTK-mediated modulation of cell morphology, Vav3F was transfected into ER2-, IR-, or IGFR-overexpressing NIH 3T3 cells and the percentages of Vav3-positive cells with different shapes with or without ligand stimulation were calculated. In the IR- and Vav3-expressing cells, insulin stimulation significantly enhanced the proportion of cells displaying lamellipodia or membrane ruffles (from 22 to 50%), but had no apparent effect on the proportion of cells displaying filopodia or microspike formation. By contrast, in IGFR- and Vav3-overexpressing cells, IGF-1 specifically promoted Vav3-mediated microspike formation (from 12 to 24%). It is interesting that activation of IR and IGFR leads to distinct Vav3-mediated morphological changes. Due to a high basal level of ER2-expressing cells displaying membrane ruffling, the experiments on the effect of Vav3 expression were not conclusive.

Oncogenic activation of Vav3 by CH or CH-AD domain truncation. It has previously been reported that the deletion of the CH and AD domains of Vav and Vav2 can lead to their constitutive activation. Expression of these truncated mutants in NIH 3T3 cells induces focus formation (25, 50, 51). To assess whether the same mutations can lead to oncogenic activation of Vav3, we checked the transforming ability of wild-type Vav3 and its CH and CH-AD domain deletion mutants in NIH 3T3 cells. As shown in Fig. 12, Vav3SH had no detectable

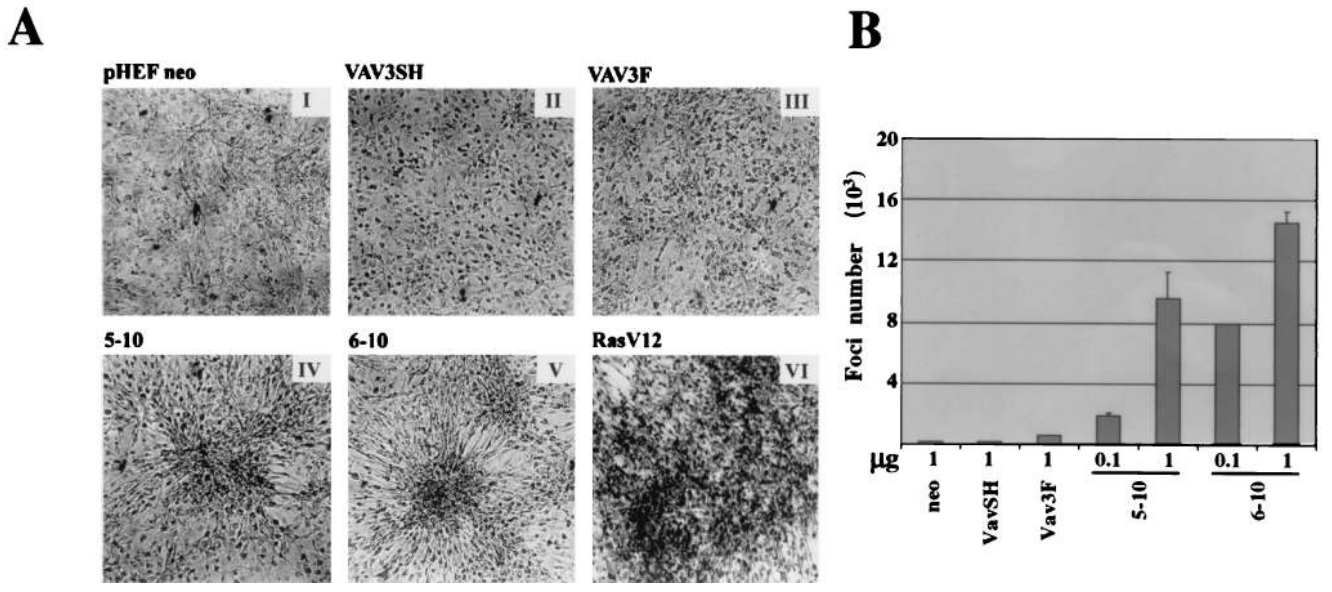

FIG. 12. N-terminal deletion mutants of Vav3-induced foci in NIH 3T3 cells. (A) The morphology of foci induced by Vav3F (III), pHEF 5-10 (IV), and pHEF 6-10 (V). NIH 3T3 cells transfected with empty vector (I), Vav3F (II), or RasV12 (VI) were included as controls and for comparison of transforming morphology. (B) The number of foci induced by full-length Vav3 and its mutants, 5-10 and 6-10.

focus-forming activity and wild-type Vav3 had only a weak focus-inducing ability. Both N-terminal truncation mutants induced very compact and elevated foci composed of small, fusiform refractile cells as opposed to the oncogenic Ras-induced foci, which are composed of wide, spreading, rounded cells. The focus-forming ability of the Vav3 mutants was investigated in three independent stocks of NIH 3T3 cells obtained from different sources with similar results. CH domain deletion unleashed the focus-forming ability of Vav3. This activity was further enhanced by the CH and AD domain deletion as seen with the 6-10 mutant. Therefore, like Vav and Vav2, N-terminal deletion of the AD domain is required for full activation of the transforming potential of Vav3. Vav3 6-10 induced close to 15×10^3 foci per μg compared to approximately 8×10^3 foci per μg induced by oncogenic Ras. The ability of Vav3 and its mutants to promote anchorage-independent growth was also examined using the soft agar growth assay. No significant Vav3-mediated colony-promoting ability was observed.

DISCUSSION

In this study, we identified Vav3 as a new Ros-associated protein in a yeast two-hybrid screen and, subsequently, in mammalian cells by coimmunoprecipitation assays. Our data show that Vav3 has a tissue expression pattern overlapping that of Ros (9). Following Ros activation, Vav3 becomes phosphorylated on its tyrosine residues. These observations suggest that Vav3 is a signaling molecule downstream of Ros. In addition, our results indicate that Vav3 also plays a role in IR-, IGFR-, and EGFR-mediated signaling pathways.

To further understand the biochemical and biological functions of Vav3, a new Vav family member, we examined its upstream regulators, associated partners, and downstream signaling pathways. Our results demonstrated that Vav3 became tyrosine phosphorylated and physically associated with EGFR, IR, and IGFR in response to the stimulation of these RPTKs. The carboxyl SH3-SH2-SH3 domains of Vav3 seem sufficient for this interaction. This is consistent with the model that Vav associates with autophosphorylated RPTKs through its SH2 domain by recognizing specific phosphotyrosine sequences in RPTKs (5). However, the interaction of Vav3 and Ros was ligand independent. There are two possibilities: (i) the basal level of tyrosine phosphorylation of Ros in the untreated EB69 cells was already sufficient for Vav3 binding, and (ii) given the fact that the SH3-SH2-SH3 domains of Vav3 are sufficient for its association with Ros, it is possible that Vav3 can interact with Ros via its SH3 rather than its SH2 domain. Whether tyrosine phosphorylation of Ros is required for the interaction remains to be investigated. In addition, Ros seems to be more potent in inducing the tyrosine phosphorylation of Vav3 than EGFR, IR, and IGFR.

In previous studies, Shc has been shown to couple to Vav protein in vivo (38). Here we report increased Vav3 association with Shc upon insulin stimulation in the presence of exogenous IR in 293T cells (Fig. 7B). The Vav protein has been shown to interact with Grb2 independent of ligand stimulation (27, 29, 46, 47, 52). It was further pointed out that this association was mediated by the N-SH3 domain of Vav and the C-SH3 domain of Grb2, therefore explaining their constitutive interaction (46, 63). However, in our study, Vav3 was associated with Grb2 upon insulin stimulation, and this interaction was further enhanced in the presence of exogenous IR. We do not know if this distinct property of Vav3 is due to its intrinsic nature or due to different cell systems used in our study versus those in the studies of others. However, our result is in agreement with the study of Ramos-Morales et al. (47), in which coimmunoprecipitation assays showed ligand-inducible interaction between Vav and Grb2.

It has been shown that PLC-γ and the p85 regulatory subunit of PI3 kinase can bind to tyrosine-phosphorylated Vav in vitro (47) and in vivo (3, 60). Consistently, our results demonstrate that PLC-γ interacted with Vav3 in a ligand-dependent manner. The interaction of Vav3 with the p85 subunit of PI3 kinase in cells was also ligand dependent, as verified by coimmunoprecipitation assay (Fig. 6B) and Vav3-associated PI3 kinase assay (data not shown).

A tyrosine-phosphorylated protein with a mass of 180 kDa

was reproducibly observed among the Vav3-associated proteins upon activation of various RPTKs. Its pronounced tyrosine phosphorylation level and frequent association with Vav3 suggest that it may play an important role in Vav3-mediated signaling function. In an attempt to identify this protein, antibodies against EGFR, IGFR, p190 Rho GAP, and IRS-1 were tested in the immunoblotting analysis. To this end, we have excluded p180 from being an IRS-1, IR, or IGFR precursor, but its identity remains unknown.

Several groups have shown that Vav and Vav2 function as GEFs for different members of the Rho/Rac family GTPases. Tyrosine phosphorylation was shown to regulate Vav GEF activity (5). It is thought that Vav family proteins couple tyrosine kinase signaling in response to distinct environmental stimuli of cells via their inducible GEF activity as well as interaction with various signaling molecules, including PLC-γ and PI3 kinase. Recently, Movilla and Bustelo (38) reported that (i) baculovirus-expressed Vav3 protein, after tyrosine phosphorylation by Lck (Y505F) in vitro, could specifically promote the GDP-GTP exchange on RhoA and RhoG and, to a lesser extent, on Rac-1 but not on Cdc42 in an in vitro GTP-GDP exchange assay; (ii) expression of Vav3(Δ1–144) or Vav3(Δ1–184) in NIH 3T3 cells led to extensive lamellipodia, membrane ruffling, and the formation of an actin ring in the cell periphery, whereas wild-type Vav3 induced morphological change only when coexpressed with activated Lck (Y505F); and (iii) wild-type Vav3, Vav3(Δ1–144), or Vav3(Δ1–184), in the presence or absence of activated Lck (Y505F), failed to induce cellular transformation in NIH 3T3 cells.

However, in our study, using GST-Rok, -Pak, and -Ack fusion polypeptides in the pull-down binding assays, we found that overexpression of wild-type Vav3 in mammalian cells led to activation of Rac-1 and Cdc42 but not RhoA, while an N-terminal truncation mutant of Vav3 promoted RhoA and Rac-1 activation but not Cdc42 activation in the same cell background. These observations suggest that Vav3 possesses GEF potential towards Cdc42, Rac-1, and RhoA. However, the RhoA GEF activity can be manifested only after deleting the N-terminal sequence that apparently negatively regulated the RhoA GEF activity, possibly by interfering with the binding of RhoA. Furthermore, our data indicate that the N-terminal sequence is required for Cdc42 GEF activity of Vav3. Several factors might contribute to the discrepancy between our observations and that of Movilla and Bustelo (38). First of all, different assay systems have been used: we detected the intracellular GTP-bound GTPases after expression of Vav3 by binding assays, whereas they used baculovirus-produced Vav3 for the in vitro GTP-GDP exchange and binding assays. Secondly, different upstream regulators may influence Vav3 substrate specificity. It is not clear whether Lck can represent the physiological upstream effector of Vav3. Different PTKs may recognize distinct tyrosine residues on Vav3. For example, our data show that IR and IGFR appear to have differential regulatory effects on Vav3-mediated GTPase activation and morphological change. It is possible that the Vav protein has the potential to activate Rho, Rac, and Cdc42 GTPases. The specificity may depend on the different upstream activators, endogenous GTPases available in a distinct cell background, and potential cofactors. Different upstream activators may modify Vav proteins at different sites, inducing different conformational changes that favor the interaction of Vav proteins with distinct GTPases. Similarly, different cells may have distinct cofactors that are needed for Vav GEF activity toward a specific GTPase. In our case, overexpression of wild-type Vav3 might have resulted in its activation by undefined upstream effectors distinct from Lck and Syk subfamily kinases and involvement of a certain cofactor that modulates Vav3 GEF activity for Cdc42 in particular. These effectors and cofactors would be excluded in the in vitro GDP-GTP exchange assay. Another explanation for the discrepancy of Vav3 and its GEF activity towards Cdc42 is that Vav3 may activate Cdc42 indirectly. For example, Vav3 can activate RhoG in vitro as shown by Movilla and Bustelo (38). RhoG in turn has been shown to activate both Rac and Cdc42. In our in vivo assay system we were not able to distinguish direct and indirect activation.

Vav and Vav2 oncogenes have been reported by several groups to induce differential morphological changes in NIH 3T3 cells. It was shown that Vav caused depolarization of fibroblasts and triggered the bundling of actin stress fibers to form parallel arrays (28), while Vav2 induced lamellipodia and marked membrane ruffles (51). Neither Vav nor Vav2 has been shown to induce filopodia or microspikes in NIH 3T3 cells. Our results show that wild-type Vav3 could induce marked morphology changes, such as membrane ruffles and microspikes, even under serum starvation conditions without coexpression of any active kinase in NIH 3T3 cells. Expression of full-length Vav3 in NIH 3T3 cells was able to induce microspike formation. This correlates with the ability of full-length Vav3 to promote the activation of Cdc42, as shown by the GST-Ack in vitro binding assay. Truncation of the CH domain of Vav3 resulted in a reduced ability to induce microspikes, but dramatically enhanced membrane ruffle formation, which is consistent with its reduced ability to induce Cdc42 activation in the GST-Ack binding assay.

Coexpression of Vav3 with different upstream regulators, such as IR and IGFR, promoted distinct Vav3-mediated morphological changes. Insulin stimulation of IR and Vav3 coexpressing cells resulted in increased Vav3-dependent membrane ruffling, whereas IGF-1 stimulation of IGFR and Vav3 coexpressing cells resulted in increased Vav3-dependent microspike formation. In contrast, the pull-down assay analysis showed only mild synergy of Vav3 with IGF-1 or insulin with respect to Cdc42 and Rac activation, respectively. The lack of synergistic effect in pull-down assays could reflect differential sensitivity of these two types of assays or that other signaling pathways activated by Vav3 but not analyzed in our study could be responsible for the morphological changes.

Finally, we show that N-terminal deletion of Vav3 leads to its oncogenic activation in focus formation. The mutants induce foci in a dose-dependent manner, and deletion of the AD domain was required for full activation of the transforming ability of Vav3. The experiment was repeated with several NIH 3T3 cell lines derived in different laboratories, with similar results.

Taken together, our study shows that Vav3, a new member of the Vav family of proteins, has structural features and biochemical properties similar to those of Vav and Vav2. These properties include tyrosine phosphorylation in response to RPTK activation and physical association with a variety of signaling molecules, such as Shc, Grb-2, PLC-γ, and PI3 kinase p85. Overexpression of wild-type Vav3 leads to activation of Rac-1 and Cdc42 and induces marked membrane ruffles and microspikes in NIH 3T3 cells. In contrast, N-terminal truncation of Vav3 results in enhanced RhoA GEF activity, oncogenic activation, and enhanced membrane ruffle formation. Different RPTKs appear to have distinct regulatory roles in Vav3-mediated GTPase activation and morphological change.

ACKNOWLEDGMENTS

We thank H. Maruta for the generous gift of the GST-Ack plasmid, B. Mayer for the GST-Pak plasmid, and P. Fedi for the anti-EGFR antibody. We would also like to thank T. Leung and E. Manser for the

Rok-α cDNA. We thank T. D. Brumeanu for several hematopoietic cell lines.

This work was supported by NIH grants CA29339 and CA55054.

REFERENCES

1. **Abe, K., K. L. Rossman, B. Liu, K. D. Ritola, D. Chiang, S. L. Campbell, K. Burridge, and C. J. Der.** 2000. Vav2 is an activator of Cdc42, Rac1, and RhoA. J. Biol. Chem. **275:**10141–10149.
2. **Bartel, P. L., C. T. Chien, R. Sternglanz, and S. Fields.** 1993. Using the two-hybrid system to detect protein-protein interactions, p. 153–179. *In* D. A. Hartley (ed.), Cellular interactions in development: a practical approach. Oxford University Press, Oxford, United Kingdom.
3. **Bertagnolo, V., M. Marchisio, S. Volinia, E. Caramelli, and S. Capitani.** 1998. Nuclear association of tyrosine-phosphorylated Vav to phospholipase C-γ 1 and phosphoinositide 3-kinase during granulocytic differentiation of HL-60 cells. FEBS Lett. **441:**480–484.
4. **Bubeck Wardenburg, J., R. Pappu, J. Y. Bu, B. Mayer, J. Chernoff, D. Straus, and A. C. Chan.** 1998. Regulation of PAK activation and the T cell cytoskeleton by the linker protein SLP-76. Immunity **9:**607–616.
5. **Bustelo, X. R.** 2000. Regulatory and signaling properties of the Vav family. Mol. Cell. Biol. **20:**1461–1477.
6. **Bustelo, X. R.** 1996. The VAV family of signal transduction molecules. Crit. Rev. Oncog. **7:**65–88.
7. **Bustelo, X. R., J. A. Ledbetter, and M. Barbacid.** 1992. Product of vav proto-oncogene defines a new class of tyrosine protein kinase substrates. Nature **356:**68–71.
8. **Chen, J., D. Heller, B. Poon, L. Kang, and L.-H. Wang.** 1991. The proto-oncogene c-ros codes for a transmembrane tyrosine protein kinase sharing sequence and structural homology with *sevenless* protein of *Drosophila melanogaster*. Oncogene **6:**257–264.
9. **Chen, J., C. S. Zong, and L.-H. Wang.** 1994. Tissue and epithelial cell-specific expression of chicken proto-oncogene c-ros in several organs suggests that it may play roles in their development and mature functions. Oncogene **9:**773–780.
10. **Collins, T. L., M. Deckert, and A. Altman.** 1997. Views on Vav. Immunol. Today **18:**221–225.
11. **Coppola, J., S. Bryant, T. Koda, D. Conway, and M. Barbacid.** 1991. Mechanism of activation of the vav protooncogene. Cell Growth Differ. **2:**95–105.
12. **Crespo, P., X. R. Bustelo, D. S. Aaronson, O. A. Coso, M. Lopez-Barahona, M. Barbacid, and J. S. Gutkind.** 1996. Rac-1 dependent stimulation of the JNK/SAPK signaling pathway by Vav. Oncogene **13:**455–460.
13. **Crespo, P., K. E. Schuebel, A. A. Ostrom, J. S. Gutkind, and X. R. Bustelo.** 1997. Phosphotyrosine-dependent activation of Rac-1 GDP/GTP exchange by the vav proto-oncogene product. Nature **385:**169–172.
14. **De Sepulveda, P., K. Okkenhaug, J. L. Rose, R. G. Hawley, P. Dubreuil, and R. Rottapel.** 1999. Socs1 binds to multiple signaling proteins and suppresses steel factor-dependent proliferation. EMBO J. **18:**904–915.
15. **Durfee, T., K. Becherer, P.-L. Chen, S.-H. Yeh, Y. Yang, A. E. Kilbrun, W.-H. Lee, and S. J. Elledge.** 1993. The retinoblastoma protein associates with the protein phosphatase type I catalytic subunit. Genes Dev. **7:**555–569.
16. **Fischer, K. D., Y. Y. Kong, H. Nishina, K. Tedford, L. E. Marengere, I. Kozieradzki, T. Sasaki, M. Starr, G. Chan, S. Gardener, M. P. Nghiem, D. Bouchard, M. Barbacid, A. Bernstein, and J. M. Penninger.** 1998. Vav is a regulator of cytoskeletal reorganization mediated by the T-cell receptor. Curr. Biol. **8:**554–562.
17. **Germani, A., F. Romero, M. Houlard, J. Camonis, S. Gisselbrecht, S. Fischer, and N. Varin-Blank.** 1999. hSiah2 is a new Vav binding protein which inhibits Vav-mediated signaling pathways. Mol. Cell. Biol. **19:**3798–3807.
18. **Gringhuis, S. I., L. F. de Leij, P. J. Coffer, and E. Vellenga.** 1998. Signaling through CD5 activates a pathway involving phosphatidylinositol 3-kinase, Vav, and Rac1 in human mature T lymphocytes. Mol. Cell. Biol. **18:**1725–1735.
19. **Hall, A.** 1998. Rho GTPases and the actin cytoskeleton. Science **279:**509–514.
20. **Han, J., B. Das, W. Wei, L. Van Aelst, R. D. Mosteller, R. Khosravi-Far, J. K. Westwick, C. J. Der, and D. Broek.** 1997. Lck regulates Vav activation of members of the Rho family of GTPases. Mol. Cell. Biol. **17:**1346–1353.
21. **Han, J., K. Luby-Phelps, B. Das, X. Shu, Y. Xia, R. D. Mosteller, U. M. Krishna, J. R. Falck, M. A. White, and D. Broek.** 1998. Role of substrates and products of PI 3-kinase in regulating activation of Rac-related guanosine triphosphatases by Vav. Science **279:**558–560.
22. **Henske, E. P., M. P. Short, S. Jozwiak, C. M. Bovey, S. Ramlakhan, J. L. Haines, and D. J. Kwiatkowski.** 1995. Identification of VAV2 on 9q34 and its exclusion as the tuberous sclerosis gene TSC1. Ann. Hum. Genet. **59:**25–37.
23. **Holsinger, L. J., D. M. Spencer, D. J. Austin, S. L. Schreiber, and G. R. Crabtree.** 1995. Signal transduction in T lymphocytes using a conditional allele of Sos. Proc. Natl. Acad. Sci. USA **92:**9810–9814.
24. **Ito, H., Y. Fukuda, K. Murata, and A. Kimura.** 1983. Transformation of intact yeast cells treated with alkali cations. J. Bacteriol. **153:**163–168.
25. **Katzav, S., J. L. Cleveland, H. E. Heslop, and D. Pulido.** 1991. Loss of the amino-terminal helix-loop-helix domain of the vav proto-oncogene activates its transforming potential. Mol. Cell. Biol. **11:**1912–1920.
26. **Katzav, S., D. Martin-Zanca, and M. Barbacid.** 1989. vav, a novel human oncogene derived from a locus ubiquitously expressed in hematopoietic cells. EMBO J. **8:**2283–2290.
27. **Kranenburg, O., M. Poland, F. P. van Horck, D. Drechsel, A. Hall, and W. H. Moolenaar.** 1999. Activation of RhoA by lysophosphatidic acid and Galpha12/13 subunits in neuronal cells: induction of neurite retraction. Mol. Biol. Cell **10:**1851–1857.
28. **Kranewitter, W. J., and M. Gimona.** 1999. N-terminally truncated Vav induces the formation of depolymerization-resistant actin filaments in NIH3T3 cells. FEBS Lett. **455:**123–129.
29. **Lee, I. S., Y. Liu, M. Narazaki, M. Hibi, T. Kishimoto, and T. Taga.** 1997. Vav is associated with signal transducing molecules gp130, Grb2 and Erk2, and is tyrosine phosphorylated in response to interleukin-6. FEBS Lett. **401:**133–137.
30. **Lopez-Lago, M., H. Lee, C. Cruz, N. Movilla, and X. R. Bustelo.** 2000. Tyrosine phosphorylation mediates both activation and downmodulation of the biological activity of Vav. Mol. Cell. Biol. **20:**1678–1691.
31. **Lu, W., and B. J. Mayer.** 1999. Mechanism of activation of Pak1 kinase by membrane localization. Oncogene **18:**797–806.
32. **Manser, E., T. H. Loo, C. G. Koh, Z. S. Zhao, X. Q. Chen, L. Tan, I. Tan, T. Leung, and L. Lim.** 1998. PAK kinases are directly coupled to the PIX family of nucleotide exchange factors. Mol. Cell **1:**183–192.
33. **Marengere, L. E., C. Mirtsos, I. Kozieradzki, A. Veillette, T. W. Mak, and J. M. Penninger.** 1997. Proto-oncoprotein Vav interacts with c-Cbl in activated thymocytes and peripheral T cells. J. Immunol. **159:**70–76.
34. **Michel, F., L. Grimaud, L. Tuosto, and O. Acuto.** 1998. Fyn and ZAP-70 are required for Vav phosphorylation in T cells stimulated by antigen-presenting cells. J. Biol. Chem. **273:**31932–31938.
35. **Miranti, C. K., L. Leng, P. Maschberger, J. S. Brugge, and S. J. Shattil.** 1998. Identification of a novel integrin signaling pathway involving the kinase Syk and the guanine nucleotide exchange factor Vav1. Curr. Biol. **8:**1289–1299.
36. **Montaner, S., R. Perona, L. Saniger, and J. C. Lacal.** 1999. Activation of serum response factor by RhoA is mediated by the nuclear factor-kappaB and C/EBP transcription factors. J. Biol. Chem. **274:**8506–8515.
37. **Montaner, S., R. Perona, L. Saniger, and J. C. Lacal.** 1998. Multiple signaling pathways lead to the activation of the nuclear factor kappaB by the Rho family of GTPases. J. Biol. Chem. **273:**12779–12785.
38. **Movilla, N., and X. R. Bustelo.** 1999. Biological and regulatory properties of Vav-3, a new member of the Vav family of oncoproteins. Mol. Cell. Biol. **19:**7870–7885.
39. **Nur-E-Kamal, M. S. A., J. M. Kamal, M. M. Qureshi, S. Iwashita, W. Montague, and H. Maruta.** 1999. The CDC42-specific inhibitor derived from ACK-1 blocks v-Ha-Ras-induced transformation. Oncogene **18:**7787–7793.
40. **Olson, M. F., N. G. Pasteris, J. L. Gorski, and A. Hall.** 1996. Faciogenital dysplasia protein (FGD1) and Vav, two related proteins required for normal embryonic development, are upstream regulators of Rho GTPases. Curr. Biol. **6:**1628–1633.
41. **Onodera, H., D. G. Motto, G. A. Koretzky, and D. M. Rothstein.** 1996. Differential regulation of activation-induced tyrosine phosphorylation and recruitment of SLP-76 to Vav by distinct isoforms of the CD45 protein-tyrosine phosphatase. J. Biol. Chem. **271:**22225–22230.
42. **O'Rourke, L. M., R. Tooze, M. Turner, D. M. Sandoval, R. H. Carter, V. L. Tybulewicz, and D. T. Fearon.** 1998. CD19 as a membrane-anchored adaptor protein of B lymphocytes: costimulation of lipid and protein kinases by recruitment of Vav. Immunity **8:**635–645.
43. **Pandey, A., A. V. Podtelejnikov, B. Blagoev, X. R. Bustelo, M. Mann, and H. F. Lodish.** 2000. Analysis of signaling complexes by mass spectrometry: identification of Vav-2 as a novel substrate of the epidermal growth factor receptor. Proc. Natl. Acad. Sci. USA **97:**179–184.
44. **Platanias, L. C., and M. E. Sweet.** 1994. Interferon alpha induces rapid tyrosine phosphorylation of the vav proto-oncogene product in hematopoietic cells. J. Biol. Chem. **269:**3143–3146.
45. **Raab, M., A. J. da Silva, P. R. Findell, and C. E. Rudd.** 1997. Regulation of Vav-SLP-76 binding by ZAP-70 and its relevance to TCR zeta/CD3 induction of interleukin-2. Immunity **6:**155–164.
46. **Ramos-Morales, F., F. Romero, F. Schweighoffer, G. Bismuth, J. Camonis, M. Tortolero, and S. Fischer.** 1995. The proline-rich region of Vav binds to Grb2 and Grb3–3. Oncogene **11:**1665–1669.
47. **Ramos-Morales, F., B. J. Druker, and S. Fischer.** 1994. Vav binds to several SH2/SH3 containing proteins in activated lymphocytes. Oncogene **9:**1917–1923.
48. **Romero, F., and S. Fischer.** 1996. Structure and function of Vav. Cell. Signal. **8:**545–553.
49. **Sander, E. E., S. van Delft, J. P. ten Klooster, T. Reid, R. A. van der Kammen, F. Michiels, and J. G. Collard.** 1998. Matrix-dependent Tiam1/Rac signaling in epithelial cells promotes either cell-cell adhesion or cell migration and is regulated by phosphatidylinositol 3-kinase. J. Cell Biol. **143:**1385–1398.
50. **Schuebel, K. E., X. R. Bustelo, D. A. Nielsen, B. J. Song, M. Barbacid, D. Goldman, and I. J. Lee.** 1996. Isolation and characterization of murine Vav2, a member of the vav family of proto-oncogenes. Oncogene **13:**363–371.
51. **Schuebel, K. E., N. Movilla, J. L. Rosa, and X. R. Bustelo.** 1998. Phosphor-

ylation-dependent and constitutive activation of Rho proteins by wild-type and oncogenic Vav-2. EMBO J. **17:**6608–6621.
52. **Song, J. S., J. Gomez, L. F. Stancato, and J. Rivera.** 1996. Association of a p95 Vav-containing signaling complex with the FcepsilonRI gamma chain in the RBL-2H3 mast cell line. Evidence for a constitutive in vivo association of Vav with Grb2, Raf-1, and ERK2 in an active complex. J. Biol. Chem. **271:**26962–26970.
53. **Song, J. S., H. Haleem-Smith, R. Arudchandran, J. Gomez, P. M. Scott, J. F. Mill, T. H. Tan, and J. Rivera.** 1999. Tyrosine phosphorylation of Vav stimulates IL-6 production in mast cells by a Rac/c-Jun N terminal kinase-dependent pathway. J. Immunol. **163:**802–810.
54. **Teramoto, H., P. Salem, K. C. Robbins, X. R. Bustelo, and J. S. Gutkind.** 1997. Tyrosine phosphorylation of the vav proto-oncogene product links FcRI to the Rac1-JNK pathway. J. Biol. Chem. **272:**10751–10755.
55. **Trenkle, T., M. McClelland, K. Adlkofer, and J. Welsh.** 2000. Major transcript variants of VAV3, a new member of the VAV family of guanine nucleotide exchange factors. Gene **245:**139–149.
56. **Turner, M., P. J. Mee, A. E. Walters, M. E. Quinn, A. L. Mellor, R. Zamoyska, and V. L. Tybulewicz.** 1997. A requirement for the Rho-family GTP exchange factor Vav in positive and negative selection of thymocytes. Immunity **7:**451–460.
57. **Uddin, S., S. Katzav, M. F. White, and L. C. Platanias.** 1995. Insulin-dependent tyrosine phosphorylation of the vav protooncogene product in cells of hematopoietic origin. J. Biol. Chem. **270:**7712–7716.
58. **Uddin, S., A. Yetter, S. Katzav, C. Hofmann, M. F. White, and L. C. Platanias.** 1996. Insulin-like growth factor-1 induces rapid tyrosine phosphorylation of the vav proto-oncogene product. Exp. Hematol. **24:**622–627.
59. **Van Aelst, L., and C. D'Souza-Schorey.** 1997. Rho GTPases and signaling networks. Genes Dev. **11:**2295–2322.
60. **Weng, W. K., L. Jarvis, and T. W. LeBien.** 1994. Signaling through CD19 activates Vav/mitogen-activated protein kinase pathway and induces formation of a CD19/Vav/phosphatidylinositol 3-kinase complex in human B cell precursors. J. Biol. Chem. **269:**32514–32521.
61. **Wilson, R., R. Ainscough, K. Anderson, C. Baynes, M. Berks, J. Bonfield, J. Burton, M. Connell, T. Copsey, J. Cooper, et al.** 1994. 2.2Mb of contiguous nucleotide sequence from chromosome III of *C. elegans*. Nature **368:**32–38.
62. **Wu, J., S. Katzav, and A. Weiss.** 1995. A functional T-cell receptor signaling pathway is required for p95vav activity. Mol. Cell. Biol. **15:**4337–4346.
63. **Ye, Z. S., and D. Baltimore.** 1994. Binding of Vav to Grb2 through dimerization of Src homology 3 domains. Proc. Natl. Acad. Sci. USA **91:**12629–12633.
64. **Zhang, R., F. Y. Tsai, and S. H. Orkin.** 1994. Hematopoietic development of vav/mouse embryonic stem cells. Proc. Natl. Acad. Sci. USA **91:**12755–12759.